Journal of Medicinal Chemistry

pubs.acs.org/jmc Article

Identification of Potent and Long-Acting Single-Chain Peptide Mimetics of Human Relaxin-2 for Cardiovascular Diseases

Sergio Mallart,* Raffaele Ingenito, Elisabetta Bianchi, Alberto Bresciani, Simone Esposito, Mariana Gallo, Paola Magotti, Edith Monteagudo, Laura Orsatti, Daniela Roversi, Alessia Santoprete, Federica Tucci, Maria Veneziano, Régine Bartsch, Claudius Boehm, Denis Brasseur, Patricia Bruneau, Alain Corbier, Jacques Froissant, Laurence Gauzy-Lazo, Vincent Gervat, Frank Marguet, Isabelle Menguy, Claire Minoletti, Marie-Françoise Nicolas, Olivier Pasquier, Bruno Poirier, Alexandre Raux, Laurence Riva, Philip Janiak, Hartmut Strobel, Olivier Duclos, and Stephane Illiano

Cite This: *J. Med. Chem.* 2021, 64, 2139−2150 Read Online

ACCESS | Metrics & More | Article Recommendations | Supporting Information

ABSTRACT: The insulin-like peptide human relaxin-2 was identified as a hormone that, among other biological functions, mediates the hemodynamic changes occurring during pregnancy. Recombinant relaxin-2 (serelaxin) has shown beneficial effects in acute heart failure, but its full therapeutic potential has been hampered by its short half-life and the need for intravenous administration limiting its use to intensive care units. In this study, we report the development of long-acting potent single-chain relaxin peptide mimetics. Modifications in the B-chain of relaxin, such as the introduction of specific mutations and the trimming of the sequence to an optimal size, resulted in potent, structurally simplified peptide agonists of the relaxin receptor Relaxin Family Peptide Receptor 1 (RXFP1) (*e.g.*, **54**). Introduction of suitable spacers and fatty acids led to the identification of single-chain lipidated peptide agonists of RXFP1, with subnanomolar activity, high subcutaneous bioavailability, extended half-lives, and *in vivo* efficacy (*e.g.*, **64**).

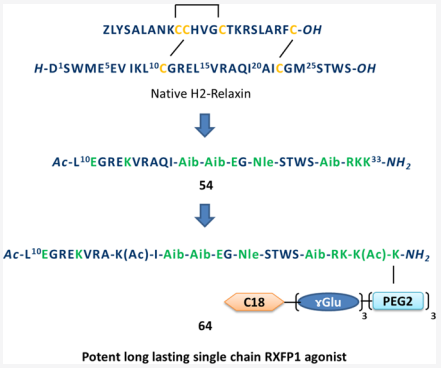

INTRODUCTION

Human relaxin-2 (H2-relaxin, referred to as relaxin from herein) is a peptide hormone member of the insulin-like family. It exerts its effects by binding to RXFP1 (Relaxin Family Peptide Receptor 1) and RXFP2 (Relaxin Family Peptide Receptor 2). These two receptors have differential tissue distributions,[1] with relaxin's vascular and anti-fibrotic activity being mediated by RXFP1.[2]

Relaxin was first identified to play a key role during pregnancy. This hormone is involved in uterus remodeling and embryo implantation, as well as in modulating hemodynamic adaptation in pregnant women.[3] The hemodynamic changes induced by relaxin improve the cardiac afterload by decreasing the vascular resistance and leading to an increase in cardiac output and glomerular filtration rates.[1]

Chronic subcutaneous (SC) relaxin infusion in rats and mice increases arterial compliance in small renal, mesenteric, uterine, and carotid arteries.[4] In conscious normotensive and hypertensive male and female rats, acute intravenous (IV) and chronic SC administration of relaxin increases the cardiac output and global arterial compliance, in addition to reducing systemic vascular resistance, without affecting the mean arterial pressure.[2] Furthermore, relaxin has anti-fibrotic properties in animal models of cardiac and kidney fibrosis.[5]

Beneficial cardiovascular effects of recombinant relaxin (serelaxin) have been demonstrated in congestive and acute heart failure patients in phase 2 clinical trials.[6] However, in phase 3 studies involving a total of 6545 patients hospitalized for acute heart failure, a 48 h IV infusion of serelaxin (30 μg per kg of body weight per day) was no more effective than placebo when measuring the incidence of death caused by the worsening of heart failure or other cardiovascular ailments.[7] One cause of this lack of efficacy might have been the short *in vivo* half-life of relaxin, which may limit the hormone's long-term therapeutic use and underlines the need for long-acting agents. Attempts to address this issue were recently reported using recombinant relaxin-bearing natural[8] or non-natural aminoacid[9−11] mutations on the A-chain. The newly introduced mutations were used to covalently modify relaxin with half-life-extending moieties such as lipids or polyethylene glycol (PEG) moieties, resulting in the discovery of long-lasting double-chain relaxin

Received: October 8, 2020
Published: February 8, 2021

https://dx.doi.org/10.1021/acs.jmedchem.0c01533
J. Med. Chem. 2021, 64, 2139−2150

analogues. More recently, mRNA therapeutic encoding for (long-lasting) relaxin was reported to have advanced in clinical development.[12]

Relaxin has a complex heterodimeric insulin-like structure that makes its chemical synthesis and purification difficult, resulting in low production yields (Figure 1).[13] The knowledge

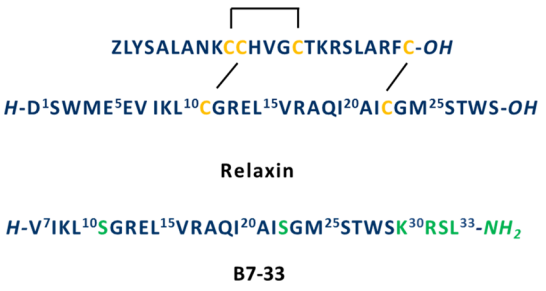

Figure 1. Structure of relaxin and B7-33. Relaxin B-chain numbering used throughout this text. In B7-33, residues highlighted in green represent the changes from native relaxin B-chain. Z, pyroglutamate residue.

of the structure−activity relationship (SAR) of relaxin-like peptides[14] has led to attempts to simplify relaxin's structure while maintaining the pharmacological activity of the hormone.[15−17] Exploiting the knowledge that relaxin activates RXFP1 primarily through the interaction of its B-chain with the high-affinity binding site located at the extracellular leucine-rich repeat (LRR) domain of RXFP1, Hossain *et al.* recently identified a single-chain peptide, derived from relaxin B-chain (B7-33), as a functional agonist of RXFP1.[18−20]

These studies demonstrated that the B-chain peptide of relaxin, in the absence of A-chain, contains the requisite elements to mediate RXFP1 activation.[18] However, B7-33 exhibited reduced potency compared to relaxin.[19] B7-33 binds recombinant RXFP1 in HEK-293T cells with a pK_i of 5.54, while relaxin exhibited a pK_i of 8.96. Similarly, the pEC$_{50}$ values for cAMP activity assays were 5.12 and 10.49 for B7-33 and relaxin, respectively.[19] Moreover, in-house studies found that B7-33 is poorly soluble in buffer at pH 7.4 and unstable in plasma (*vide infra*).

We report here on our efforts to discover long-lasting RXFP1 agonists. Stepwise modification of the relaxin B-chain by introduction of mutations, identification of the optimal peptide length, and incorporation of suitable spacers and fatty acids resulted in short single-chain peptide agonists of the relaxin receptor RXFP1, displaying sub-nanomolar activity and high SC bioavailability, with extended half-lives and *in vivo* efficacies.

RESULTS AND DISCUSSION

The goal of the present study was to identify potent single B-chain relaxin analogues that displayed a sustained duration of action, suitable for once daily administration. Detailed below are a number of synthetic strategies carried out to reach this objective. In native relaxin, the B-chain adopts an α-helical structure that packs against the A-chain. The support provided by this packing enables the key residues of the B-chain-binding cassette (Arg13, Arg17, Ile20) to be optimally oriented for interaction with the LRR domain of RXFP1.[21,22] Our hypothesis was that the single B-chain peptide, devoid of the structural constraint provided by the A-chain, is flexible in solution and has a low tendency to populate the helical conformation, as suggested by circular dichroism (CD) (Supporting Information Figure S1) and NMR (Supporting Information Figures S2 and S3) spectroscopy. As a consequence of the conformational freedom of the unbound B-chain, a large entropic penalty is likely paid upon binding of the peptide to the RXFP1 receptor. It is this energetic penalty which probably explains the observed weaker affinity and potency of B7-33 compared to those of native relaxin.[18,19] To overcome this limitation, our initial objective was to stabilize the active conformation of the B-chain in the absence of A-chain structural support, by introducing conformational constraints that could increase the propensity of the B-chain to adopt an α-helical secondary structure. In addition, we explored the optimal length of the B-chain that leads to the delivery of potent and stable peptides. Several non-natural amino acids were also introduced at strategic positions within the sequence to investigate the increasing *in vivo* stability. Finally, in order to improve peptide pharmacokinetics (PK), fatty acids of varying lengths were covalently linked *via* diverse linkers to the peptides.

Alanine and Amino Isobutyric Acid Scan. To investigate the individual contribution of each amino acid to potency, a series of C-terminal amide peptides were prepared where several positions of the B7-33 sequence were mutated to either alanine (Ala) or amino isobutyric acid (Aib) (abbreviated as U in the tables for sequence alignment). Alanine mutation was used because of its non-bulky, chemically inert side chain, while the α-dimethyl amino acid Aib stabilizes the conformation of helical peptides.[23] Moreover, Aib also protects adjacent peptide bonds from proteolytic cleavage. Both properties of Aib were exploited during peptide optimization. The effect of each mutation was assessed by testing the peptides in a cAMP assay performed in OVCAR5 cells, an ovarian cancer cell line expressing endogenous RXFP1. To establish the SAR in this series, peptides of purity ranging from 91 to 98% were tested and results are reported as a range of activities in Table 1. Starting from the N-terminus, mutation to Ala of positions, Leu10 (**4a**),

Table 1. Influence of a Single Ala or Aib Mutation on the Activation of RXFP1 Receptor by Peptides Derived from B7-33[a]

Position	7	8	9	10	11	12	13	14	15	16	17	18	19	20	21	22	23	24	25	26	27	28	29	30	31	32	33
Sequences*	V	I	K	L	S	G	R	E	L	V	R	A	Q	I	A	I	S	G	M	S	T	W	S	K	R	S	L
Cpd. #	1	2	3	4	5	6	7	8	9	10	11	12	13	14	15	16	17	18	19	20	21	22	23	24	25	26	27
a : Ala**	ns	ns				ns			ns	ns							ns		ns					ns			
b : Aib**							ns	ns			ns	ns		ns				ns	ns			ns	ns	ns	ns	ns	ns

[a]Potency range for cAMP measurement in OVCAR5 cells. EC$_{50}$ values were obtained after full concentration-dependent response to each compound, and each peptide was tested in duplicate 1−8 times. * All peptides are C-terminal amides. ** Each cell represents a compound with Ala (a) or Aib (b) mutation at the indicated position (ns = compound not synthesized). Compounds were classified with different color codes for activity range with respect to EC$_{50}$ of parent compound (B7-33, EC$_{50}$ = 1 641 ± 350 nM, E_{max} = 90%), orange: EC$_{50}$ > 5 × EC$_{50}$ (B7-33), light yellow: 0.5−5 × EC$_{50}$ (B7-33), green: EC$_{50}$ < 0.5 × EC$_{50}$ (B7-33).

https://dx.doi.org/10.1021/acs.jmedchem.0c01533
J. Med. Chem. 2021, 64, 2139−2150

Table 2. cAMP Assay in OVCAR5 Cells and cIep of Single B-Chain Analogues from B7-33 and B5-33 Series Bearing Several Mutations[a]

Cpd.	Sequences*	EC_{50} ± SEM nM (Emax%)**	cIep*** (net Charge)
	5 10 15 20 25 30 33		
28	..VIKLSGRELVRAQIAISGMSTWSKRSL	929±248 (70%)	12.8 (+4)
29	..VIKLSGRELVRAQIAISGMSTWSKRKK	522±107 (89%)	12.8 (+6)
30	..VIKLSGRELVRAQIUISGMSTWSKRSL	708±71 (78%)	12.8 (+4)
31	..VIKLSGRELVRAQIUISGMSTWSKRKK	202±72 (90%)	12.8 (+6)
32	..VIKLSGRELVRAQIAUSGMSTWSKRKK	393±50 (102%)	12.8 (+6)
33	..VIKLSGRELVRAQIUUSGMSTWSKRKK	92.1± 41.3 (99%)	12.8 (+6)
34	..VIKLEGREKVRAQIUISGMSTWSKRKK	46.0±11 (98%)	12.3 (+6)
35	..VIKLSGRELVRAQIUIEGMSKWSKRKK	146±47 (102%)	12.3 (+6)
36	..VIKLEGREKVRAQIUIEGMSKWSKRKK	54.0±35.0 (95%)	11.8 (+6)
37	..VIKLEGREKVRAQIUUEGMSKWSKRKK	17.0±5.0 (99%)	11.8 (+6)
38	..VIKLEGREKVRAQIUUEGMSKWSURKK	19.5±0.5(99%)	11.7 (+5)
39	EEVIKLSGRELVRAQIAISGMSTWSKRKK	897±168 (92%)	11.0 (+4)
40	EEVIKLSGRELVRAQIUISGMSTWSKRSL	498±288 (86%)	10.7 (+2)
41	EEVIKLSGRELVRAQIUISGMSTWSKRKK	143±2.8(94%)	11.0 (+4)
42	EEVIKLSGRELVRAQIAUSGMSTWSKRSL	200±130 (91%)	10.7 (+2)
43	EEVIKLSGRELVRAQIAUSGMSTWSKRKK	32.0±20.1 (95%)	11.0 (+4)
44	EEVIKLSGRELVRAQIUUSGMSTWSKRKK	37.0±5.0(94%)	11.0 (+4)
45	EEVIKLEGREKVRAQIUISGMSTWSKRKK	124±49 (98%)	11.3 (+4)
46	EEVIKLSGRELVRAQIUIEGMSKWSKRKK	230±8.2 (101%)	11.3 (+4)
47	EEVIKLEGREKVRAQIUIEGMSKWSKRKK	45.0±15.0 (97%)	11.1 (+4)
48	EEVIKLEGREKVRAQIUUEGMSKWSURKK	17.0±0.5 (95%)	10.9 (+3)
49	EEVIKLEGREKVRAQIUUEGMSTWSURKK	17.8±2.1 (99%)	10.7 (+2)

[a]*All peptides are N-terminal acetylated and C-terminal amides, U = Aib. **cAMP assay in OVCAR5 cells, each peptide tested in duplicate 2−8 times each. EC_{50} values were obtained after full concentration-dependent response to each compound. The E_{max} % represents the max value for each compound compared to the max value obtained with 100 nM relaxin. ***Calculated isoelectric point and net charge at pH 7.5 using EMBOSS explorer http://www.bioinformatics.nl/emboss-explorer/.

Ser11 (**5a**), Gln19 (**13a**), Ile22 (**16a**), Ser26 (**20a**), Thr27 (**21a**), Ser29 (**23a**), Arg31 (**25a**), Ser32 (**26a**), and Leu33 (**27a**) yielded an improvement in potency compared to that of parent compound (B7-33, EC_{50} = 1 641 ± 350 nM, E_{max} = 90%), demonstrating that several positions are amenable to mutation that do not diminish the peptide activity. Mutations R13A (**7a**), R17A (**11a**), and I20A (**14a**) resulted in a significant decrease in potency which confirms the importance of the arginine-binding cassette in B7-33 analogues.[19] Surprisingly, G24A (**18a**) mutation was also detrimental to activity. As this residue does not contribute to the binding of relaxin to RXFP1, the drop in potency suggests that this residue is important for the peptide to adopt biologically active conformation. The Aib scan identified several mutations that produced an improvement in potency: G12Aib (**6b**), Q19Aib (**13b**), A21Aib (**15b**), I22Aib (**16b**), and S23Aib (**17b**).

Peptide Sequence Optimization and Identification of Novel B10-33 Series. Modifications in B-chain sequences of varied lengths brought about improvements in peptide potency, solubility, and plasma stability. Table 2 shows the results of the cAMP functional readout used to test the peptide activity. In order to decrease the net charge, improve the plasma stability, and increase the helical content, all peptides were acetylated at the N-terminus.[24] Ser32 and Leu33 were subsequently replaced by two C-terminal lysine residues to increase the peptide solubility. These transformations were well tolerated, as demonstrated by **29** (EC_{50} = 522 ± 107 nM) having comparable potency to B7-33 and its acetylated analogue **28** (EC_{50} = 929 ± 248 nM). In order to counterbalance the increased net charge of the peptide following the introduction of the two C-terminal lysines, compound **29** was elongated at the N-terminus with the two glutamic acid residues that are found in native relaxin (**39**, EC_{50} = 897 ± 168 nM). Further modifications were performed in parallel on **29** (B7-33 series) and **39** (B5-33 series). A21Aib or I22Aib mutations identified as permissive in the Aib scan gave rise to **31** (EC_{50} = 202 ± 728 nM) and **32** (EC_{50} = 393 ± 50) in the B7-33 series and **41** (EC_{50} = 143 ± 2.8 nM) and **43** (EC_{50} = 32.0 ± 20 nM) in the B5-33 series. The I22Aib mutation produced the largest increase in potency and this in combination with the A21Aib mutation gave rise to **44** (EC_{50} = 37.0 ± 5.0 nM). We postulate that the increased potency of **44** is likely due to conformational stabilization induced by the two Aib in positions 21 and 22, along with the two lysines in positions 32 and 33, with this latter modification having previously been

https://dx.doi.org/10.1021/acs.jmedchem.0c01533
J. Med. Chem. 2021, 64, 2139−2150

shown to increase peptide conformational stability.[25,26] These transformations were also applied to the B7-33 series with a comparable improvement in potency, as exemplified by **33** (EC_{50} = 92.1 ± 43.3 nM). In **43** and **44**, Glu5 is in an (*i*, *i* + 4) relationship with Lys9. The increased potency of these two compounds is likely due to improved peptide conformational stabilization brought about by a salt bridge between Glu5 and Lys9.[27] With this assumption in mind, systematic introduction of putative Glu−Lys salt bridges at positions (*i*, *i* + 4) along the helical region of the relaxin B-chain (Gly12−Ser23, Supporting Information Figure S3), was carried out. Introducing these modifications in the B5-33 series led to the generation of potent peptides such as **45** (S11E−L15K; EC_{50} = 124 ± 49 nM) and **46** (S23E−T27K; EC_{50} = 230 ± 8.2 nM). Combining all of these mutations gave rise to **47** (EC_{50} = 45.0 ± 15.0 nM). Similar results were obtained for the B7-33 series, for example, **36** (EC_{50} = 54.0 ± 35.0 nM). Incorporating the I22Aib mutation in **36** improved the peptide potency (**37**, EC_{50} = 17.0 ± 5.0 nM).

The poor solubility of the B-chain of relaxin (B1-29) in aqueous medium hampers the chemical synthesis of native relaxin[13] and limits the ability of B1-29 to activate RXFP1.[28] In spite of its increased net charge at neutral pH,[19] B7-33 also had limited equilibrated solubility at pH 7.4 and was unstable in rat and human plasma (Table 3).

Table 3. Solubility and Rat/Human Plasma Stability of Representative Peptides[a]

Cpd.	series	aqueous solubility* (mg/mL)		plasma stability (% remaining after 4 h of incubation)	
		pH 4.5	pH 7.4	Human	rat
B7-33	7−33	1.9	0.014	3	2
31	7−33	5.7	4.6	54	37
36	7−33	4.8	3.8	79	29
37	7−33	5.1	5.3	58	37
49	5−33	2.8	2.4	80	60
51	10−33	n.d.	n.d.	79	24
53	10−33	6.1	5.8	93	101
54	10−33	3.3	2.9	64	55
57	10−33	4.0	4.0	74	60

[a]*Equilibrated solubility obtained in 50 mM buffer (acetate pH 4.5 or phosphate pH 7.4) after 24 h.

The modifications described above gave rise to soluble peptides, but stability in human and rat plasma, although improved (Table 3, **31**, **36**, and **37**), was still limited. This increase in solubility and plasma stability could be attributed to the presence of the positively charged KRKK patch at the C-terminus, as has been observed in other peptides bearing a $(Lys)_6$ patch such as Lixisenatide.[25,26] Identification of the metabolites generated from proteolytic catabolism upon incubation of **31** with plasma revealed Leu10−Ser11, Ala18−Gln19, Aib21−Ile22, and Ser29−Lys30 to be the most labile peptide bonds (Supporting Information Table S3). We hypothesized that the K30Aib mutation might protect the plasma-labile peptide bond (position 29−30). Peptides bearing this mutation were as potent as their parent counterparts (B7-33 series; **38** *vs* **37**). In B5-33 series, **48** appeared to be one of the most potent peptides (EC_{50} = 17.0 ± 0.5 nM). Interestingly, mutating Lys27 in **48** back to a Thr27 in **49**, as found in native relaxin, maintained the potency (Table 2).

In summary, there was a 100-fold improvement in the EC_{50} of optimized peptides in the B7-33 and B5-33 series with respect to their starting point (B7-33). Peptides in these series display good solubility at physiological pH and acceptable plasma stability. However, from the chemical manufacturing and control stand point, the sequence EEVIKL of the B5-33 series was problematic, leading to amino acid deletions and resulting in poor yields in large-scale peptide syntheses. In addition, catabolic hot spots were found at peptide bonds Lys9−Leu10 and Leu10−Glu11 (data not shown). In order to solve these issues and identify the optimal peptide length, peptides were further truncated from the N-terminus up to position Leu10 yielding the novel B10-33 series (Table 4).

Remarkably, peptides from the B10-33 series display similar potencies in the OVCAR5-cAMP assay compared to the B5-33 and B7-33 peptides. The most potent peptides in the B10-33 series were **51** and **53** (EC_{50} = 14.0 ± 8.0 nM for both peptides). These results constitute the first demonstration that shortening the relaxin B-chain up to position 10 gives rise to potent peptides, provided that additional conformational constraints are introduced to counterbalance the lack of the A-chain. The bioisosteric M25Nle mutation was also tolerated (**54**, EC_{50} = 12.0 ± 3.0 nM), whereas the Q19K(Ac) mutation decreased potency 3 times (**56**, EC_{50} = 45 ± 15 nM). In addition, Lys33 acetylation was well tolerated (**55**, EC_{50} = 32 ± 12 nM and **57**, EC_{50} = 18 ± 15 nM) indicating that this modification is permissive in modified B-chain peptides. Compound **53** was stable in plasma for up to 4 h (Table 3), while its analogues with M25Nle mutation and/or the presence of K(Ac) residues, **54** and **57** were less stable. Compound **54** combined good on-target potency and plasma stability and was selected for PK in rat and *in vivo* pharmacological assays.

Molecular Dynamics Simulations. Molecular dynamics simulations were performed to rationalize the increased potencies of the modified peptides and to gain further insights into peptide structuration (Figure 2).

The central core of the peptide between Arg13 and Glu23 is maintained in a stable helicoidal conformation during molecular dynamics simulation. Several salt bridges that contribute to the tertiary structure of the peptide and those that are located in the non-helicoidal N- and C-termini are also maintained during the simulation. Two salt bridges formed within the Arg13−Glu14−Arg17 motif located at the N-terminus of the helix ensure that the two arginine residues of the RXFP1-binding cassette (Arg13 and Arg17) are correctly ordered and oriented. A salt bridge between Glu11 and Lys15 structures the N-terminal loop in a hairpin-like conformation. Glu23 is involved in a bridge with Arg31, rather than the expected interaction with Lys27, which was designed to act as an (*i*, *i* + 4) electrostatic staple. These two salt bridges do not contribute to helix stabilization but rather structure and orient both ends of the peptide toward the central core. The N-terminus hairpin-like conformation confers a compact structure to the peptide, which prevents unfavorable contacts with the RXFP1-LRR domain. The salt bridge formed between Glu23−Arg30 at the C-terminus of the peptide could facilitate Trp28 binding to the LRR-LDLa module linker. This interaction is thought to play an important role in RXFP1 activation.[22]

***In Vivo* Evaluation of Compound 54.** The *in vivo* activity of the peptides was assessed by analyzing their effect on the well-documented chronotropic effect of relaxin in rodents.[2,29−31] Relaxin induces a chronotropic effect in rodents (not in humans) *via* PKA activation and inhibition of the transient

https://dx.doi.org/10.1021/acs.jmedchem.0c01533
J. Med. Chem. 2021, 64, 2139−2150

Table 4. cAMP Assay in OVCAR5 Cells and cIep of Single B-Chain Analogues from 10−33 Series Bearing Several Mutations[a]

Cpd.	Sequences*	$EC_{50} \pm SEM$ nM (Emax%)**	cIep (net Charge)***
	10 15 20 25 30 33		
50	LEGREKVRAQ IUIEGM SKWSKRKK	43±19 (91%)	11.7 (+5)
51	LEGREKVRAQ IUUEGM SKWSKRKK	14±8 (99%)	11.7 (+5)
52	LEGREKVRAQ IUUEGM STWSKRKK	23±1 (99%)	11.7 (+4)
53	LEGREKVRAQ IUUEGM STWSURKK	14±8 (99%)	11.6 (+3)
54	LEGREKVRAQ IUUEGNleSTWSURKK	12±3 (99%)	11.6 (+3)
55	LEGREKVRAQ IUUEGNleSTWSURKK(Ac)	32±12 (96%)	11.5 (+2)
56	LEGREKVRAK(Ac) IUUEGNleSTWSURKK	45±15 (95%)	11.6 (+3)
57	LEGREKVRAK(Ac) IUUEGNleSTWSURKK(Ac)	18±15 (93%)	11.5 (+2)

[a]*All peptides N-terminal-acetylated C-terminal amide, U = Aib, Nle = Norleucine, L-2-aminohexanoic acid, K(Ac) = Nε-acetyl-L-lysine. **cAMP assay in OVCAR5 cells, each peptide tested in duplicate 2−8 times each. ***Calculated isoelectric point and net charge at pH 7.5 using EMBOSS explorer http://www.bioinformatics.nl/emboss-explorer/.

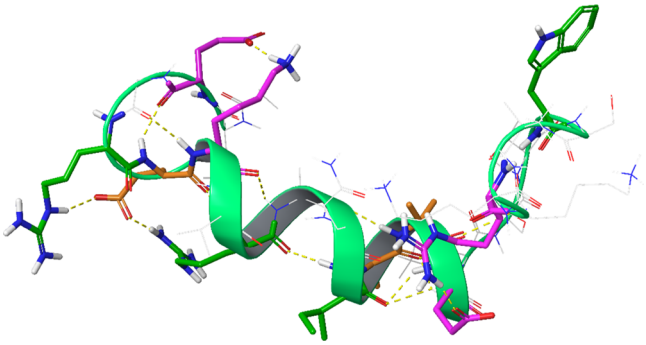

Figure 2. Molecular dynamics simulated structure of **54**. Only heavy atoms are represented. Residues whose roles are described here have a stick representation. Magenta: residues involved in maintaining the backbone conformation. Green: residues involved in binding to RXFP1. Orange: Glu14.

potassium outward current resulting in action potential prolongation.[30] This effect has been used for the *in vivo* characterization of the small molecule RXFP1 agonist, ML290.[31] A pithed rat model was used to evaluate the *in vivo* activity and potency of **54** in comparison with relaxin (Figure 3). This model allows control mechanisms (*i.e.*, baroreceptor reflex) that can dampen the effect of drugs on the heart rate (HR) or peripheral resistance to be excluded.

Following IV bolus injection, relaxin produced a strong chronotropic effect in pithed rats (+ 60% HR increase at 10 μg/kg (1.6 nmol/kg)). Compound **54** increased the HR by + 40% at 300 μg/kg (108 nmol/kg). These values are equivalent to the potency ratio of **54** and relaxin in the cAMP test on rat RXFP1 expressed in HEK cells (r-RXFP1-HEK293, Table 5). Compound **54** is thus a potent single-chain peptide agonist of RXFP1 with relaxin-like biological activity *in vivo*. However, although the *in vivo* half-life of **54** (0.32 h) in rats after IV administration was comparable to that of relaxin (0.46 h), this value was still limiting (Supporting Information Table S4). As a consequence to this finding, additional peptide modification was explored with the aim of improving this parameter.

Optimization of B10-33 Series Peptide *In Vivo* Half-Life. Among the numerous strategies that have previously been used to improve the *in vivo* duration of action of therapeutic peptides is the increase of hydrodynamic radius, to decrease the

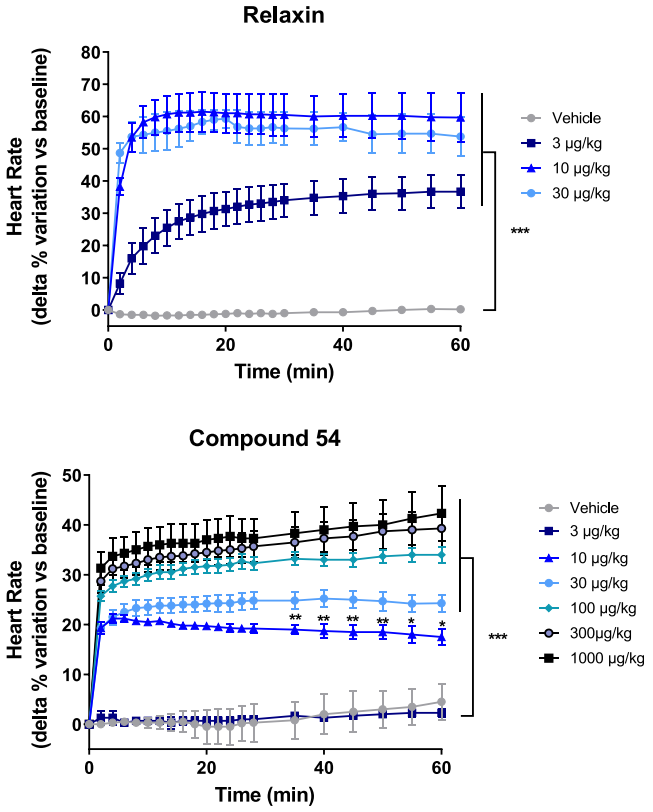

Figure 3. Chronotropic effect—% increase in HR—of relaxin and **54** after IV bolus administration in pithed rats (male S.D. rats; relaxin, $n = 6$ per dose; **54**, $n = 6$ per dose, except 3 μg/kg and 1000 μg/kg doses, $n = 3$). *P*-values: ***$p < 0.001$, **$p < 0.01$, and *$p < 0.05$ *vs* vehicle. Two-way analysis of variance type with repeated measures on one factor. Post hoc contrast analysis versus vehicle on the factor group at a fixed factor time with Bonferroni−Holm adjustment. *P*-values for each dose and time point are summarized in Supporting Information Table S10.

renal clearance.[32] This can be achieved by the covalent modification of peptides with the polymer PEG or albumin-binding moieties, in particular, fatty acids.[32−35] Recently, long-lasting relaxin analogues have been obtained by attaching 20k PEG[9,11] or fatty acids[10] preferably at the A-chain or B-chain N-termini, but it was still to be demonstrated whether such strategy

https://dx.doi.org/10.1021/acs.jmedchem.0c01533
J. Med. Chem. 2021, 64, 2139−2150

Table 5. cAMP Production Following RXFP1 Activation in OVCAR5 Cells and Rat RXFP1 (r- RXFP1) Expressed in HEK296 Cells with Relaxin and 54[a]

	cAMP assay, EC_{50} nM (E_{max} %)	
compound	OVCAR5 cells	r-RXFP1−HEK296 cells
Relaxin	0.42 ± 0.3 (100%)	0.5 ± 0.1(100%)
54	12 ± 3 (99%)	5.3 ± 1.0 (83%)

[a]Each peptide tested in duplicate 2−5 times each. Relaxin and **54** have comparable potency on rat RXFP1 expressed in HEK296 cells and human RXFP1 (OVCAR5). Cellular activity is not affected by HSA or RSA for these non-lipidated peptides.

could be successfully applied to the linear peptide derived from the B-chain of relaxin. In the present study, it was found that the N-ε acetylation of Lys33 was well tolerated (Table 3, **54** *vs* **55** and **56** *vs* **57**). Position 33 (the C-terminus) was thus chosen as a site for peptide modification.

Figure 4 outlines the general strategy that was followed to improve the *in vivo* half-life of the B10-33 series. Lys33 or Lys34, if applicable, was covalently modified with side chains bearing fatty acids of various lengths. A linker was introduced to modulate the distance between the peptide core and the albumin-binding moiety.

In vivo half-life enhancement of lipidated peptides is dependent on their binding to albumin through the fatty acid moiety. In spite of potentially increasing the *in vivo* half-life, it was conceivable that albumin bound to lipidated peptides could hinder the engagement of the LRR-binding cassette with RXFP1, and thus, prevent or reduce receptor activation and *in vivo* efficacy. The activity on OVCAR5 cells in the presence of 2% human serum albumin (HSA) was measured, and the albumin shift (AS = cAMP assay EC_{50} 2% HSA/EC_{50} w/o HSA ratio) was monitored (see the footnote in Table 6).

Lipidation of compounds **53** to **57** (B10-33 series) at Lys33 or additional Lys34 gave rise to the constructs shown in Table 6.

The potency of C16 and C18 lipidated peptides was either maintained or increased over parent peptides (Table 4). An example of this finding is seen in the acylated form of **53**. Modification of this peptide at Lys33 with a −γE−γE−γE−C16 side chain (−γE: gamma-glutamyl; C16: palmityl) moiety gave rise to **58** which had reduced the net charge and cIep values (4.8 *vs* 11.6 and −1 *vs* +3, respectively). The potency of **58** in the cAMP assay on OVCAR5 cells was maintained (EC_{50} = 17.6 ± 8.1 nM) but was shifted above the maximal test concentration when the peptide was preincubated with 2% HSA (EC_{50} > 3 μM). When a PEG12 linker was inserted between positions 32 and 33 of the peptide backbone of **58**, an increase of potency was observed in the quiescent medium and in the presence of HSA (**59**, EC_{50} = 3.6 ± 2.0 nM, EC_{50} 2% HSA = 270 ± 120 nM). M25Nle mutation was well tolerated (**60**, EC_{50} = 3.2 ± 2.1 nM). Interestingly, replacement of the C16 fatty acid by a C18 fatty acid chain in **60** increased the potency and decreased the albumin shift (AS) (**61**, EC_{50} = 1.0 ± 0.9 nM, AS ×31). Insertion of Nε-acetyl lysine (K(Ac)) between positions 32 and 33 in **61**, in combination with isosteric Q19K(Ac) mutation gave rise to a low nanomolar compound even in the presence of 2% albumin (**62**, EC_{50} = 0.6 ± 0.4 nM, EC_{50} 2% HSA = 9.0 ± 4.0 nM). A similar increase in potency was observed when the same transformation was made on **58** giving rise to **63** (EC_{50} = 1.0 ± 0.6 nM, AS ×87). In **63**, replacement of the C16 fatty acid by a C18 fatty acid chain increased the potency but had no effect on albumin shift (**64**, EC_{50} = 0.2 ± 0.1 nM, AS ×92). An analogue of **64**, with −$(PEG2)_3$ moved to the peptide backbone proved to be equally potent (**65**, EC_{50} = 0.1 ± 0.1 nM, AS ×198). Large albumin shifts were observed for compounds bearing the −$(PEG2)_3$− linkers compared to **61** and **62** which combined the PEG12 linker and the C18 lipid moiety. The use of −$(PDGA)_3$− linkers which has a comparable length to the −PEG12− linker [−$(PDGA)_3$−: 57 atoms, −PEG12−: 43 atoms] gave rise to a potent compound but still with a high albumin shift (**66**, EC_{50} = 0.4 ± 0.2 nM, AS ×61). Surprisingly, in **63** and **64**, replacing C16 or C18 fatty acid moieties by their corresponding linear fatty diacids gave rise to compounds with reduced potency (**67**, EC_{50} = 809 ± 20 nM, **68**, EC_{50} = 368 ± 76 nM).

In summary, lipidation of **53** resulted in compounds with improved potency in the cAMP OVCAR5 assay. The SAR in

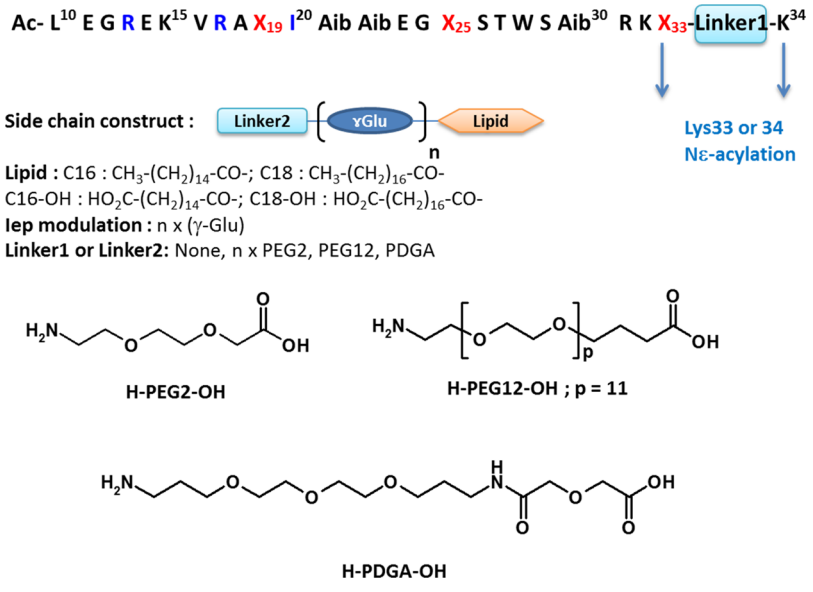

Figure 4. Half-life optimization strategy: C-terminal lipidation of B10-33 series at Lys33 or an additional Lys at position 34, with constructs including a linker, a γ-Glu spacer, and a lipid. Structures of PEG2, PEG12, and PDGA linkers.

https://dx.doi.org/10.1021/acs.jmedchem.0c01533
J. Med. Chem. 2021, 64, 2139−2150

Table 6. cAMP Production Following RXFP1 Activation in OVCAR5 Cells with Lipidated B10-33 Series Peptides[a]

Sequence = Ac-LEGREKVRA-X_{19}-I-Aib-Aib-EG-X_{25}-STWS-Aib-RK-X_{33}-Linker1-K(side chain)-NH_2									
Cpd.	X_{19}	X_{25}	X_{33}	linker1	side chain:	cAMP assay* EC_{50} nM (E_{max} %)		AS**	T1/2 (h)***
						OVCAR5 cells	OVCAR5 cells + 2% HSA**		
58	Gln	met	none	none	-$(\gamma E)_3$-C16	17.6 ± 8.1(97%)	>3 μM	>170	4.3
59	Gln	met	none	PEG12	-$(\gamma E)_3$-C16	3.6 ± 2.0 (88%)	270 ± 120 (88%)	75	8.9
60	Gln	Nle	none	PEG12	-$(\gamma E)_3$-C16	3.2 ± 2.1 (74%)	ND		6.4
61	Gln	Nle	none	PEG12	-$(\gamma E)_3$-C18	1.0 ± 0.9 (79%)	31 ± 16 (80%)	31	4.8
62	K(Ac)	Nle	K(Ac)	PEG12	-$(\gamma E)_3$-C18	0.6 ± 0.4 (95%)	9.0 ± 4.0 (84%)	15	4.3
63	K(Ac)	Nle	K(Ac)	none	-$(PEG2)_3$-$(\gamma E)_3$-C16	1.0 ± 0.6 (80%)	87 ± 30 (96%)	87	5.7
64	K(Ac)	Nle	K(Ac)	none	-$(PEG2)_3$-$(\gamma E)_3$-C18	0.2 ± 0.1 (89%)	18.4 ± 5.8 (89%)	92	3.9
65	K(Ac)	Nle	K(Ac)	$(PEG2)_3$	-$(\gamma E)_3$-C18	0.1 ± 0.1 (88%)	19.8 ± 4.6 (82%)	198	3.4
66	K(Ac)	Nle	K(Ac)	$(PDGA)_3$	-$(\gamma E)_3$-C18	0.4 ± 0.2 (88%)	24.5 ± 13 (85%)	61	3.96
67	K(Ac)	Nle	K(Ac)	none	-$(PEG2)_3$-$(\gamma E)_3$-C16-OH	809 ± 20 (70%)	>2 μM		ND
68	K(Ac)	Nle	K(Ac)	none	-$(PEG2)_3$-$(\gamma E)_3$-C18-OH	368 ± 76 (75%)	>2 μM		ND

[a]* cAMP assay in OVCAR5 cells, each peptide tested in duplicate 2−18 times. ** Peptides were incubated with 2% HSA for 30 min prior to conducting the cAMP assay. ** AS: albumin shift (EC_{50} 2% HSA/EC_{50} w/o HSA). *** $T_{1/2}$ *in vivo* half-life in rat 1 mg/kg IV. PK parameters are given in Supporting Information Table S5

lipidated peptides mirrored the SAR observed in non-lipidated peptides of Table 5. Insertion of linkers of various lengths and lipid composition resulted in nanomolar or sub-nanomolar compounds with low albumin shifts when preincubated with HSA. While the albumin shift could not be correlated to the *in vivo* half-life in rat PK studies (Table 6, $T_{1/2}$ column), they provided interesting insights on the behavior of these constructs in *in vivo* assays, as described in the following section. It has not been possible to clearly elucidate the origin of the observed increase in potency for C16 and C18 lipidated peptides. One possible explanation could be an increase in peptide conformational stability. Indeed, analysis of the secondary structure by CD spectroscopy (Supporting Information Figure S5 and Table S6) revealed that the addition of a lysine at position 34 in **57**, modified with suitable linkers and fatty acids, resulted in an increase in the proportion of helical structure present in the studied sample from 5% (**57**) to 21% (**63**) and 29% (**64**). These findings are consistent with previous reports[36] and suggest that fatty acids contribute to helix stability. Moreover, the linker and fatty acid could play an additional role in RXFP1 activation by filling the space that is occupied by the A-chain of relaxin, thereby stabilizing lipidated single B-chain peptide−RXFP1 complexes. In this context, the loss of activity observed with **67** and **68** could be due to unfavorable interaction between the fatty diacid chain ω-carboxylic acid moiety and the receptor.

***In Vitro* and *In Vivo* Characterization Studies.** Improved plasma and blood stability were observed for lipidated peptides compared to their non-lipidated counterparts, as shown in Table 7. Importantly, aqueous solubility at physiological pH was not compromised by lipidation. In addition, chemical and physical stability studies were conducted with **64** in buffers compatible with *in vivo* pharmacological studies at 4, 25, and 40 °C. Under these conditions, **64** was chemically stable for 4 weeks with no sign of aggregation or fibrillation (Supporting Information Table S7).

The PK studies in rats showed that compounds from Table 6 displayed *in vivo* half-lives ranging from 3.4 to 7.9 h (Table 6 and Supporting Information Table S5), which are significantly longer than **54** and comparable to that of liraglutide, a GLP1-R agonist that is dosed once a day.[33] Longer *in vivo* half-lives were obtained with peptides containing C16 fatty acid side chains (**59**, $T_{1/2}$ = 8.9 h, and **60**, $T_{1/2}$ = 6.4 h). The corresponding C18 peptide (**61**, $T_{1/2}$ = 4.8 h) had a significantly shorter half-life.

Table 7. Solubility and Rat/Human Plasma or Blood Stability of Representative Peptides[a,b]

Cpd.	type	aqueous solubility* (mg/mL) at pH 7.4	human plasma stability** % remaining at 4 h	rat plasma stability** % remaining at 4 h
53	NL	5.8	93	101
58	C16	ND	91***	93***
57	NL	4.0	74	60
62	C18	5.4	96	80
63	C16	ND	87***	79***
64	C18	11.4	111	114

[a]Non-lipidated (NL) peptides and C16 or C18 lipidated peptides. [b]Compound **53** is the non-lipidated analogue of **58**. Compound **57** is the non-lipidated analogue of **63** and **64**. *Equilibrated solubility obtained in 50 mM buffer (phosphate pH 7.4) after 24 h. **Stability in plasma except ***stability in blood.

The same finding was observed for **63** (C16; $T_{1/2}$ = 5.7 h) when compared to **64** (C18; $T_{1/2}$ = 3.9 h). This pattern could not be easily rationalized. As a general observation, it is known that for lipidated peptides, the albumin shift and the PK profile are influenced by a series of phenomena such as peptide oligomerization[37] and the relative binding affinity to albumin versus the biological target.[34] These are dynamic processes influenced by the concentration and formulation. In addition, the *in vivo* behavior of lipidated peptides is influenced by other factors including the metabolism and binding to blood components besides albumin.

Subcutaneous bioavailability of these peptides ranged from 47% (Table S5, **63**) to 100% (Table S5, **61**). Metabolite identification in **61** rat PK samples showed limited catabolism indicating that modifications of the peptide backbone, as described above, resulted in proteolytically stable peptides (Supporting Information Figure S6 and Table S8).

Compound **59**, which displayed a long *in vivo* half-life but moderate cellular activity, and **64** with low nanomolar activity on OVCAR5 cells in the presence of HSA were selected for further *in vivo* evaluation (Figure 5). Compound **59** was assessed on rat RXFP1 using HEK293 cells expressing rat RXFP1 (r-RXFP1-HEK293, cAMP assay) and proved to be active in this assay (EC_{50} = 0.9 ± 1.0 nM, E_{max} 79%, albumin shift with rat serum albumin (RSA) ×33) which is in the same range as h-

https://dx.doi.org/10.1021/acs.jmedchem.0c01533
J. Med. Chem. 2021, 64, 2139−2150

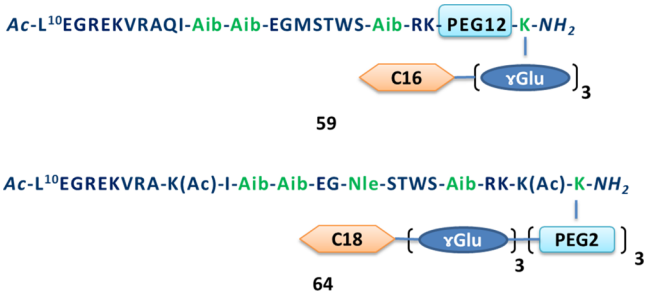

Figure 5. Structures of **59** and **64**.

RXFP1. As reported above for relaxin and **54**, the chronotropic effect in pithed rat was used as a screening model for *in vivo* RXFP1 activation. Figure 6A, shows the maximal chronotropic effect obtained with **59** and **64** at the four doses studied (see also Supporting Information Figure S7).

Compounds **59** and **64** elicit a dose-dependent chronotropic effect in pithed rats (Figure 6A). Despite being more potent *in vitro,* in the quiescent medium, compared to **54**, lipidated analogues displayed a lower maximal effect (26 and 30% at 1000 μg/kg IV bolus for **64** and **59,** respectively *vs* 43% for **54**). The reduced *in vivo* activity is probably due to a lower plasma free fraction with lipidated peptides compared to that of non-lipidated peptides, as reflected by the observed albumin shift in cellular assays. A lag time to reach maximal HR increase was also observed for lipidated peptides (Supporting Information Figure S7) compared to the non-lipidated equivalent **54** (Figure 3). Among the peptides tested in this assay, **59** displayed the slowest onset. However, the chronotropic effect in pithed rats is an acute model used for compound triage. Chronic models are needed for the selection of a lead compound. It is in this context that better PK parameters and improved *in vivo* residence time of **59** (Figure 6B) compared to those of analogues **61**, **62**, and **64**, can compensate for the slow onset and reduced maximal *in vivo* effect (Supporting Information Figure S7).

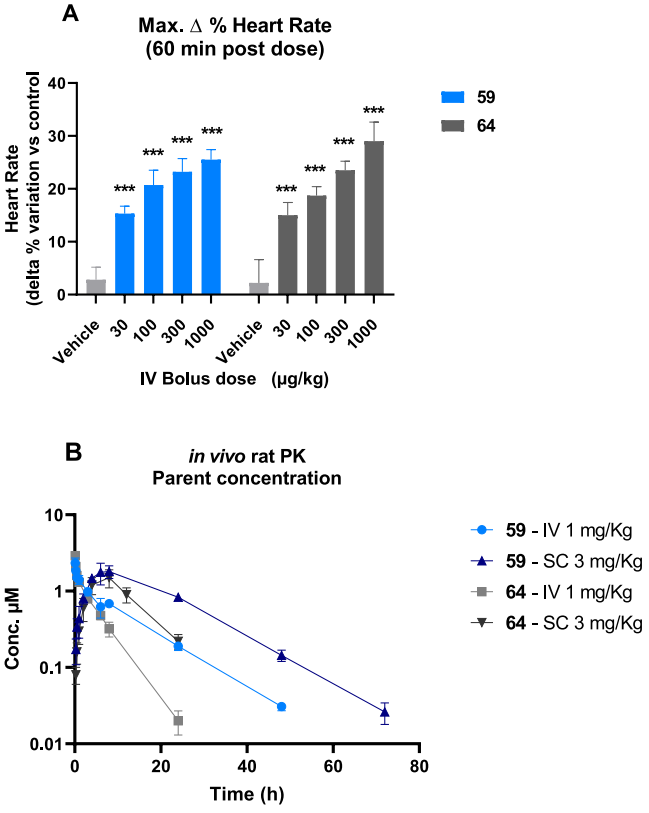

Figure 6. (A): Chronotropic effect—% increase in HR—after IV bolus administration (male S.D. rats; **59**, $n = 6$ per dose, except 1000 μg/kg dose, $n = 4$; **64**, $n = 6$ per dose). Expressed as Δ% variation versus control. *P*-values: ***$p < 0.001$, **$p < 0.01$, *$p < 0.05$ *vs* vehicle. Two-way analysis of variance type with repeated measures on one factor. Post-hoc contrast analysis *vs* vehicle on factor group at a fixed factor time with Bonferroni–Holm adjustment. Statistical analysis for each dose and time point are summarized in Supporting Information Table S10. (B): Rat PK of **59** and **64**, IV 1 mg/kg, SC 3 mg/kg. (male S.D. rats, $n = 3$ for each admin. route).

In summary, the lipidated peptides **59**, **61**, **62**, and **64** were identified as long-lasting RXFP1 agonists and constitute the first examples of single B-chain analogues of relaxin with high target potency and balanced *in vivo* half-lives and efficacies. In contrast to relaxin, these peptides were found to be selective for RXFP1 versus RXFP2 (Supporting Information Table S9). Selectivity was also good with respect to other relaxin family peptide receptors (Supporting Information Table S9). Owing to their distinct profiles, these peptides qualify as a potent, long-lasting RXFP1 agonist lead compounds in the search for treatment of various diseases, including heart failure, pulmonary hypertension, scleroderma, or hepatorenal syndrome.

CONCLUSIONS

Potent long-lasting agonists of RXFP1 have been identified using several strategies to increase the potency and stability of the relaxin B-chain peptide. An initial introduction of several mutations with natural or non-natural amino acids to improve the secondary and tertiary peptide structure led to peptides with low nanomolar potency in the cellular assay and increased metabolic stability in plasma. Several peptides in the B7-33 and B5-33 series with low nanomolar activity in the OVCAR5 cell cAMP assay were obtained after mutation of positions 21, 22, and 30 with Aib and introduction of Glu/Lys pairs at positions 11/15 and 23/27. Molecular dynamics simulations contributed to rationalizing the gain in potency by identifying key salt bridges that induce conformational stabilization of the peptide, enabling key residues to be correctly orientated for binding to RXFP1. Guided by metabolite identification studies, the peptide sequence was trimmed down to the novel B10-33 series, which corresponds to the shortest peptide ever reported that is capable of potently activating RXFP1. Modification of the C-terminal lysine side chain with linkers and lipids of various lengths resulted in a further increase in potency. Furthermore, these peptides had measured *in-vivo* half-lives of between 3 and 9 h in rats after IV dosing and bioavailability compatible with once daily SC administration. The chronotropic effect in pithed rats was used as a screening assay to assess the *in vivo* efficacy of lipidated and non-lipidated peptides. While non-lipidated peptides elicited a strong and rapid chronotropic effect, lipidated peptides displayed a slower onset, probably due to a lower free fraction in plasma following albumin binding.

In summary, the translation of the benefit of RXFP1 activation, from preclinical models to the clinic, has been limited by the short half-life of relaxin, which has limited its therapeutic use to IV perfusion. The new class of RXFP1 agonists described in this report, with long-lasting properties and compatible with once daily SC administration in patients, could open the door to new treatments for chronic fibrosis and cardiovascular diseases.

https://dx.doi.org/10.1021/acs.jmedchem.0c01533
J. Med. Chem. 2021, 64, 2139–2150

EXPERIMENTAL SECTION

Materials and Methods. *Molecular Dynamics Simulation of Peptides.* Molecular modeling was conducted using Schrodinger tools: Maestro, Macromodel, and Desmond (Schrödinger Release 2019−3: MacroModel, Schrödinger, LLC, New York, NY, 2019) using the OPLS3 force field. Peptides were generated in their fully extended conformation. The resulting structures were energy-minimized with MacroModel and then subjected to molecular dynamics.

Each peptide was introduced into a cubic water box with 12 Å buffer, using the SPC solvent model, supplemented with NaCl of 0.15 M concentration. Each system underwent a 250 ns molecular dynamics simulation, after undergoing the standard relaxation protocol, with a 2 fs time-step, an *NPT* ensemble, and a target temperature of 298 K.

Synthesis of Peptides. All peptides were prepared by solid-phase peptide synthesis using the Fmoc strategy. Rink amide resins were loaded in the range of 0.2 to 0.4 mmol/g. Peptide synthesis was carried out using either the CEM Liberty Blue peptide synthesizer (microwave heating) or the Gyros Protein Technology Tribute or the Symphony peptide synthesizers (room-temperature peptide synthesis).

Peptides were acetylated at the end of the solid-phase synthesis using 5 equiv of acetic anhydride and 10 equiv of DIEA in DMF for 30 min. The synthesis of C-terminal lipidated peptides was carried out using orthogonally protected lysines [Fmoc-Lys(Dde)-OH, Fmoc-Lys-(ivDde)-OH, Fmoc-Lys(alloc)-OH, or Fmoc-Lys(Mtt)-OH], which were incorporated at appropriate positions. Following peptide assembly, the protecting group was selectively removed using hydrazine hydrate 5% v/v in DMF (Dde or ivDde), phenylsilane, or dimethylamine borane (10 eqiv) and $Pd(PPh_3)$ 10 mol% in DCM (Alloc) or TFA 1% v/v in DCM (Mtt). Completion of the reaction was monitored by cleaving the synthesized peptide from an aliquot part of resin beads, followed by ultraperformance liquid chromatography (UPLC) analysis. Side chains were modified using the Fmoc peptide synthesis strategy. At the end of assembly, peptides were cleaved from the solid support by treatment with a solution of TFA/phenol/H_2O/tri-isopropyl-silane (87.5%/5%/5%/2.5%) for 2 h, followed by precipitation in cold methyl-*tert*-butyl ether and a fresh ether wash. Peptides were purified by RP-HPLC on a C4 or C18 column using 0.1% TFA acetonitrile and water as solvents. The purity (95%) and identity of compounds were determined by UPLC-MS. For *in vivo* testing, the TFA counterion was exchanged with an acetate salt using an anion-exchange resin (*e.g.*, Bio-Rad AGx1, acetate form). The effectiveness of ion exchange was determined by ^{19}F NMR (400 MHz) spectroscopy ns 1028.

Analytical data (UPLC-MS) of all peptides are reported in Supporting Information Table S1

In Vitro cAMP Assay. All peptides were tested in duplicate 2−8 times each. The assay was performed in OVCAR5 cells expressing endogenous RXFP1. The homogenous time-resolved fluorescence (HTRF) technology was used to detect cAMP. In summary, OVCAR5 cells were grown in regular medium (Roswell Park Memorial Institute, RPMI) containing 10% fetal calf serum (FCS) and 1% antibiotics (penicillin/streptomycin). Before the experiments, the cells were detached with Accutase and incubated for 40 min at 37 °C with 1 mM 3-isobutyl-1-methylxanthine (IBMX). The cells were then distributed in 384 black well plates containing increasing concentrations of the test peptide in a fixed volume of medium (without FCS). After 30 min incubation at 37 °C in a humid incubator containing 5% CO_2, the reaction was stopped by adding a fixed volume of a solution containing a lysis buffer, cAMP-D2 (cAMP labeled with the dye d2), and the anti-cAMP antibody linked to europium, used for cAMP detection. Following HTRF measurements conducted on a fluorimeter, activation curves were generated by plotting the intracellular value of cAMP versus $\log_{10}$ of the compound concentration. The concentration corresponding to 50% activation (EC_{50}) was calculated by non-linear regression using the sigmoidal dose−response (variable slope) equation with Prism 5 software. E_{max} % is determined as the maximal intracellular value of cAMP for the test compound (upper limit of cAMP *vs* concentration curve) divided by the maximal intracellular value of cAMP for H2-relaxin determined in the same test multiplied by 100. $E_{max}\% = 100 \times [\text{cAMP test Cpd}]/[\text{cAMPH2-Rlx}]$.

Cellular Assay in the Presence of HSA. All peptides were tested in duplicate 2−8 times each. The same OVCAR5 cAMP assay protocol was followed; however, cells were incubated for 40 min at 37 °C with 1 mM IBMX and 2% HSA. Peptide solutions were prepared in medium + 2% HSA and incubated for 30 min prior to cell distribution. The same protocol was used when RSA was used for compounds tested in HEK cells expressing stable rat RXFP1.

Pithed Rat Model. All animal studies were performed in accordance with European Community Standards on the Care and Use of Laboratory Animals and approved by the IACUC of Sanofi R&D. Animals were purchased from Janvier Labs-France. Male Sprague-Dawley (S.D.) rats aged 8−10 weeks (250−300 g) were anesthetized with sodium pentobarbital (60 mg/kg, i.p.). After tracheal cannulation, rats were pithed using an appropriate metal rod and rapidly connected to the ventilator (64 inspiration/min, 3 mL/min). Vagus nerves were then sectioned, and a Millar probe was positioned at the left carotid to record the arterial pressure (AP) and HR (IOX2 software, EMKA). Compounds were administered by IV route (slow bolus) through a 22G Cathlon at the jugular vein. After a 15−20 min stabilization period, a 2 min baseline was recorded before starting the compound injection, and then AP and HR were followed over a 60 min period. Data were averaged every 2 min for the first 30 min and then averaged every 5 min. Data are expressed as delta % of the stabilization period.

CD Spectroscopy. CD spectra were recorded at 20 °C using quartz cells with 0.1 cm path length on a JASCO J-710 CD spectropolarimeter (JASCO International Co. Ltd.). Measurements were recorded within the 260−185 nm spectral range, using a 1 nm bandwidth, with an 8 s time constant and a 5 nm/min scan speed and averaged for two acquisitions. The peptide concentration was 0.1 mg/mL in 10 mM sodium phosphate buffer (pH 7.4). The Bestsel algorithm was used to extract the secondary structure contents:[38] doi: 10.1093/nar/gky497.

Solubility Determination. The study solutions at pH 7.4 and 4.5 were 50 mM phosphate and acetate buffers, respectively. Peptide stock solutions at 2, 6, or 10 mg/mL concentrations in the appropriate buffer were prepared. The sample vials were mixed (rock and roll shaker) for ∼19 h. Aliquots of 300 μL of peptide solution were filtered through a Millipore "Solvinert" plate (0,45 μm—PTFE hydrophilic). Peptide solubility was then determined using UPLC analysis [Waters Acquity UPLC system with a diode array detector, Waters Peptide Column CSH C18 (130 Å; 1.7 μm; 50 × 2.1 mm)], by comparing the UV peak areas of a 0.2 μL injection of the filtrate with that obtained with a stock solution at a concentration of 1.2 mg/mL in DMSO (based on % purity). The sample volume injection ranged from 0.2 to 2 μL.

Stability in Rat or Human Plasma. The medium used for the study was either rat or human plasma containing the anticoagulant sodium or lithium heparin. A stock solution of peptide was prepared in 50 mM phosphate buffer (pH 7.4) such that the final concentration was100 μM. The plasma (950 μL) was pre-incubated for 5 min at 37 °C before 50 μL of compound stock solution was added to obtain a final compound concentration of 5 μM. The tube was vortexed and 150 μL of plasma was transferred into an Eppendorf tube for each time point reading. Each time point (0−1 and 0−4 h) was carried out in duplicate for both human and rat plasma samples. Reaction termination at the time points was carried out by the addition of 600 μL of acetonitrile containing 1% TFA to the plasma samples. The mixture was vortexed and then centrifuged for 10 min at 14,600 rpm. The supernatant (200 μL) was dried under N_2, reconstituted with 200 μL of H_2O/CH_3CN 98/2 + 0.1% FA + 50 ng/mL labetalol, and analyzed using the analytical method applied in the solubility studies.

To determine the amount of peptide remaining after incubation, the peak areas of the target compound at t_0 and at each time point were compared. The resultant "% peptide remaining" was calculated using the following equation

$$\%\ \text{remaining peptide} = [(\text{peak area peptide at each time point})/\text{peak area peptide } t_0] \times 100$$

Stability is expressed as "% peptide remaining".

https://dx.doi.org/10.1021/acs.jmedchem.0c01533
J. Med. Chem. 2021, 64, 2139−2150

Acceptance criteria: The test compounds were considered stable if precision was ~ 15% and the recovery was within 85−115%.

Pharmacokinetics. All animal studies were performed in accordance with the European Community Standards on the Care and European Community standard on the care and use of laboratory animals Use of Laboratory Animals and approved by the IACUC of Sanofi R&D. Animals were purchased from Janvier Labs-France. Male Sprague Dawley (S.D.) rats aged 8−10 weeks (250−300 g, n = 3 per administration route) were dosed with the study peptide at a dose of 1 mg/kg IV and 3 mg/kg SC as a solution in PBS (0.2 and 0.6 mg/mL, respectively). Blood samples were collected from individual animals at the following time points: 0.083, 0.25, 0.5, 1, 3, 6, 8, 24, 48, and 72 h (IV route) and 0.25, 0.5, 1, 2, 4, 8, 12, 24, 48, and 72 h (SC route). The plasma samples (EDTA anticoagulant), prepared from blood, were extracted using a protein precipitation method and then analyzed using liquid chromatography-high-resolution mass spectrometry (LC-HRMS). PK parameters were calculated by fitting the plasma concentration−time data to a non-compartmental model using Watson LIMS 7.5 software. Values below the limit of quantification were replaced by zero for subsequent calculations. Plasma metabolite/catabolite identification was carried out by LC-HRMS for sample analysis and Biopharma Finder 2.0 (Thermo Scientific) or UNIFI Scientific Information System (Waters) for data mining.

■ ASSOCIATED CONTENT

Supporting Information

The Supporting Information is available free of charge at https://pubs.acs.org/doi/10.1021/acs.jmedchem.0c01533.

Analytical data (UPLC-MS) for all peptides; CD spectra of peptides B7-33, **30**, and **31**; NMR $\Delta C_\alpha - \Delta C_\beta$ versus residue position in relaxin B-chain B7-33, **31** and **36**; NMR dynamics-predicted order parameter S^2 values versus residue number for relaxin B-chain, B7-33 and **31**; stability of B7-33 and **31** in human or rat plasma; metabolite identification (Met. ID) main catabolism sites for B7-33 and **31** in human or rat plasma; rat PK parameters for relaxin, **54**, **58**−**63**, and **65**−**69** after IV and SC administration; CD spectra of peptides; helicity determination and comparison with cAMP production following RXFP1 activation in OVCAR5 cells for **57**, **63**, **64**, and **69**; time course of appearance and decay of metabolites in rat PK of **61**; and chronotropic effect in pithed rats for **59**, **61**, **62**, and **64** (PDF)

List of simplified molecular input line entry specification (SMILES) for all synthesized compounds, their EC_{50} in cAMP assay in OVCAR5 cells, SEM, and E_{max} values (CSV)

■ AUTHOR INFORMATION

Corresponding Author

Sergio Mallart − *Integrated Drug Discovery, Sanofi R&D, Chilly Mazarin 91385, France;* orcid.org/0000-0003-1846-8683; Email: Sergio.mallart@sanofi.com

Authors

Raffaele Ingenito − *Peptides and Small Molecules R&D Department, IRBM Spa, Rome 00 071, Italy;* orcid.org/0000-0002-8292-6346

Elisabetta Bianchi − *Peptides and Small Molecules R&D Department, IRBM Spa, Rome 00 071, Italy;* orcid.org/0000-0002-5302-6912

Alberto Bresciani − *Department of Translational Biology, IRBM Spa, Rome 00 071, Italy;* orcid.org/0000-0003-4491-603X

Simone Esposito − *DMPK, IRBM Spa, Rome 00 071, Italy;* orcid.org/0000-0003-3991-0637

Mariana Gallo − *Structural Biology, IRBM Spa, Rome 00 071, Italy*

Paola Magotti − *Peptides and Small Molecules R&D Department, IRBM Spa, Rome 00 071, Italy*

Edith Monteagudo − *DMPK, IRBM Spa, Rome 00 071, Italy*

Laura Orsatti − *DMPK, IRBM Spa, Rome 00 071, Italy;* orcid.org/0000-0002-5430-9965

Daniela Roversi − *Peptides and Small Molecules R&D Department, IRBM Spa, Rome 00 071, Italy*

Alessia Santoprete − *Peptides and Small Molecules R&D Department, IRBM Spa, Rome 00 071, Italy*

Federica Tucci − *Peptides and Small Molecules R&D Department, IRBM Spa, Rome 00 071, Italy*

Maria Veneziano − *DMPK, IRBM Spa, Rome 00 071, Italy*

Régine Bartsch − *Integrated Drug Discovery, Sanofi R&D, Chilly Mazarin 91385, France*

Claudius Boehm − *Industrial Affairs, iCMC, Sanofi-Aventis R&D, Frankfurt 65926, Germany*

Denis Brasseur − *Integrated Drug Discovery, Sanofi R&D, Chilly Mazarin 91385, France*

Patricia Bruneau − *Integrated Drug Discovery, Sanofi R&D, Chilly Mazarin 91385, France*

Alain Corbier − *Cardio-Vascular and metabolism, Sanofi R&D, Chilly Mazarin 91385, France*

Jacques Froissant − *Integrated Drug Discovery, Sanofi R&D, Chilly Mazarin 91385, France*

Laurence Gauzy-Lazo − *Integrated Drug Discovery, Sanofi R&D, Chilly Mazarin 91385, France;* orcid.org/0000-0002-7109-7052

Vincent Gervat − *Integrated Drug Discovery, Sanofi R&D, Chilly Mazarin 91385, France*

Frank Marguet − *Integrated Drug Discovery, Sanofi R&D, Chilly Mazarin 91385, France;* orcid.org/0000-0002-6206-8284

Isabelle Menguy − *Integrated Drug Discovery, Sanofi R&D, Chilly Mazarin 91385, France*

Claire Minoletti − *Integrated Drug Discovery, Sanofi R&D, Chilly Mazarin 91385, France;* orcid.org/0000-0002-0161-9820

Marie-Françoise Nicolas − *Preclinical Development Sciences, Sanofi R&D, Vitry sur Seine 94400, France*

Olivier Pasquier − *DMPK France, Sanofi R&D, Alfortville 94140, France*

Bruno Poirier − *Cardio-Vascular and metabolism, Sanofi R&D, Chilly Mazarin 91385, France;* orcid.org/0000-0001-6748-1732

Alexandre Raux − *Integrated Drug Discovery, Sanofi R&D, Chilly Mazarin 91385, France*

Laurence Riva − *Cardio-Vascular and metabolism, Sanofi R&D, Chilly Mazarin 91385, France*

Philip Janiak − *Cardio-Vascular and metabolism, Sanofi R&D, Chilly Mazarin 91385, France;* orcid.org/0000-0002-7902-2514

Hartmut Strobel − *Peptides and Small Molecules R&D Department, IRBM Spa, Rome 00 071, Italy*

Olivier Duclos − *Integrated Drug Discovery, Sanofi R&D, Chilly Mazarin 91385, France*

Stephane Illiano − *Cardio-Vascular and metabolism, Sanofi R&D, Chilly Mazarin 91385, France;* orcid.org/0000-0001-9196-0493

https://dx.doi.org/10.1021/acs.jmedchem.0c01533
J. Med. Chem. 2021, 64, 2139−2150

Complete contact information is available at:
https://pubs.acs.org/10.1021/acs.jmedchem.0c01533

Author Contributions

The manuscript was written through contributions of all authors. All authors have given approval to the final version of the manuscript.

Notes

The authors declare no competing financial interest.

■ ACKNOWLEDGMENTS

We would like to thank Corinne Rousselle, Corinne Véronique, and Sylvie Calvo-Vicente for technical assistance in peptide purification; Sonia Del Rizzo, Martina Di Geronimo, Roberto Iaccarino, and Pasqualina Punzi for technical assistance in synthesis and purification; Nadia Gennari for assistance in the screening assays; Stéphanie Brot Angelique Lasbleiz and Sylvie Rochcongar for peptide solubility studies; and Dr. Kwame Amaning for help in proofreading. Dr. Ram Dharanipragada and Dr. Roy Vaz are deeply acknowledged for helpful discussions.

■ ABBREVIATIONS

B5-33, B7-33, and B10-33 series, peptides derived from the native relaxin B-chain with additional four residues from the pro-relaxin C-peptide (KRSL); Aib, amino isobutyric acid; Alloc, allyl-oxy-carbonyl; cIep, calculated isoelectric point; C16 (lipid), $CH_3-(CH_2)_{14}-CO-$; C18 (lipid), $CH_3-(CH_2)_{16}-CO-$; C16−OH (lipid), $HO_2C-(CH_2)_{14}-CO-$; C18−OH (lipid), $HO_2C-(CH_2)_{16}-CO-$; CMC, chemistry manufacturing and control; DIEA, diisopropylethyl amine; Dde, 1-(4,4-dimethyl-2,6-dioxocyclohexylidene)-ethyl; γ-E, γ-Glu, gamma glutamyl residue; ivDde, l-(4,4-dimethyl-2,6-dioxocyclohex-1-ylidene)-3-methylbutyl; K(Ac), Nε-acetyl lysine; LDLa, low-density lipoprotein a; LRR domain, leucine-rich repeat domain; Mtt, 4-methyl-trityl; Nle, norleucine; OVCAR5, ovarian cancer cell line; $Pd(PPh_3)$, tetrakis-triphenylphosphine palladium (0); Rlx, relaxin; H2-relaxin, relaxin-2; RP-HPLC, reverse-phase high-performance liquid chromatography; RSA, rat serum albumin; RXFP1(2), relaxin family peptide receptor 1(2); Z, pyroglutamate residue

■ REFERENCES

(1) Halls, M. L.; Bathgate, R. A. D.; Sutton, S. W.; Dschietzig, T. B.; Summers, R. J. International union of basic and clinical pharmacology. XCV. Recent advances in the understanding of the pharmacology and biological roles of relaxin family peptide receptors 1-4, the receptors for relaxin family peptides. *Pharmacol. Rev.* **2015**, *67*, 389−440.

(2) Sarwar, M.; Du, X.-J.; Dschietzig, T. B.; Summers, R. J. The actions of relaxin on the human cardiovascular system. *Br. J. Pharmacol.* **2017**, *174*, 933−949.

(3) Conrad, K. P.; Shroff, S. G. Effects of relaxin on arterial dilation, remodeling, and mechanical properties. *Curr. Hypertens. Rep.* **2011**, *13*, 409−420.

(4) Danielson, L. A.; Conrad, K. P. Time course and dose response of relaxin-mediated renal vasodilation, hyperfiltration, and changes in plasma osmolality in conscious rats. *J. Appl. Physiol.* **2003**, *95*, 1509−1514.

(5) Sasser, J. M. The emerging role of relaxin as a novel therapeutic pathway in the treatment of chronic kidney disease. *Am. J. Physiol.* **2013**, *305*, R559−R565.

(6) Filippatos, G.; Teerlink, J. R.; Farmakis, D.; Cotter, G.; Davison, B. A.; Felker, G. M.; Greenberg, B. H.; Hua, T.; Ponikowski, P.; Severin, T.; Unemori, E.; Voors, A. A.; Metra, M. Serelaxin in acute heart failure patients with preserved left ventricular ejection fraction: results from the RELAX-AHF trial. *Eur. Heart J.* **2014**, *35*, 1041−1050.

(7) Metra, M.; Teerlink, J. R.; Cotter, G.; Davison, B. A.; Felker, G. M.; Filippatos, G.; Greenberg, B. H.; Pang, P. S.; Ponikowski, P.; Voors, A. A.; Adams, K. F.; Anker, S. D.; Arias-Mendoza, A.; Avendaño, P.; Bacal, F.; Böhm, M.; Bortman, G.; Cleland, J. G. F.; Cohen-Solal, A.; Crespo-Leiro, M. G.; Dorobantu, M.; Echeverría, L. E.; Ferrari, R.; Goland, S.; Goncalvesová, E.; Goudev, A.; Køber, L.; Lema-Osores, J.; Levy, P. D.; McDonald, K.; Manga, P.; Merkely, B.; Mueller, C.; Pieske, B.; Silva-Cardoso, J.; Špinar, J.; Squire, I.; Stępińska, J.; Van Mieghem, W.; von Lewinski, D.; Wikström, G.; Yilmaz, M. B.; Hagner, N.; Holbro, T.; Hua, T. A.; Sabarwal, S. V.; Severin, T.; Szecsödy, P.; Gimpelewicz, C. Effects of serelaxin in patients with acute heart failure. *N. Engl. J. Med.* **2019**, *381*, 716−726.

(8) Muppidi, A.; Lee, S. J.; Hsu, C.-H.; Zou, H.; Lee, C.; Pflimlin, E.; Mahankali, M.; Yang, P.; Chao, E.; Ahmad, I.; Crameri, A.; Wang, D.; Woods, A.; Shen, W. Design and synthesis of potent, long-acting lipidated relaxin-2 analogs. *Bioconjugate Chem.* **2019**, *30*, 83−89.

(9) Kraynov, V.; Knudsen, N.; Hewet, A.; De Dios, K.; Pinkstaff, J.; Sullivan, L. Relaxin Variants and Conjugates for Therapeutic Use. U.S. Patent 20,130,237,481 A1, 2013.

(10) Dubowchik, G. M.; Gudmundsson, O. S.; Han, X.; Lawrence, R. M.; Lipovsek, D.; Madsen, C. S.; Mapelli, C.; Morin, P. E.; Myers, M. C. Modified Relaxin Polypeptides Comprising Non-Naturally Encoded Amino Acid(s) and Linked to a Pharmacokinetic Enhancer and Uses Thereof. U.S. Patent 20,180,222,960 A1, 2018.

(11) Kraynov, V.; Knudsen, N.; Hewet, A.; De Dios, K.; Pinkstaff, J.; Sullivan, L. Relaxin Variants Containing Non-Natural Amino Acids and their Preparation and Use as Promoters of Angiogenesis. WO 2012024452 A2, 2012.

(12) Xia, Z.; Ticho, B.; Briancon-Eris, N.; Dousis, A.; De Picciotto, S.; Presnyak, V.; Hoge, S.; McFadyen, I.; Benenato, K.; Kumarasinghe, E. S. Polynucleotides Encoding Relaxin and Uses for the Treatment of Fribrosis and Cardiovascular Disease. WO 2017201340 A2, 2017.

(13) Hossain, M. A.; Wade, J. D. Synthetic relaxins. *Curr. Opin. Chem. Biol.* **2014**, *22*, 47−55.

(14) Hossain, M. A.; Bathgate, R. A. D. Challenges in the design of insulin and relaxin/insulin-like peptide mimetics. *Bioorg. Med. Chem.* **2018**, *26*, 2827−2841.

(15) Belgi, A.; Bathgate, R. A. D.; Kocan, M.; Patil, N.; Zhang, S.; Tregear, G. W.; Wade, J. D.; Hossain, M. A. Minimum active structure of insulin-like peptide 5. *J. Med. Chem.* **2013**, *56*, 9509−9516.

(16) Haugaard-Kedström, L. M.; Shabanpoor, F.; Hossain, M. A.; Clark, R. J.; Ryan, P. J.; Craik, D. J.; Gundlach, A. L.; Wade, J. D.; Bathgate, R. A.; Rosengren, K. J. Design, synthesis, and characterization of a single-chain peptide antagonist for the relaxin-3 receptor RXFP3. *J. Am. Chem. Soc.* **2011**, *133*, 4965−4974.

(17) Hojo, K.; Hossain, M. A.; Tailhades, J.; Shabanpoor, F.; Wong, L. L. L.; Ong-Pålsson, E. E. K.; Kastman, H. E.; Ma, S.; Gundlach, A. L.; Rosengren, K. J.; Wade, J. D.; Bathgate, R. A. D. Development of a single-chain peptide agonist of the relaxin-3 receptor using hydrocarbon stapling. *J. Med. Chem.* **2016**, *59*, 7445−7456.

(18) Bathgate, R. A. D.; Hossain, M. A.; Wade, J. D. Modified Relaxin B Chain Peptides and Therapeutic Uses Thereof. WO 2015157829 A1, 2015.

(19) Hossain, M. A.; Kocan, M.; Yao, S. T.; Royce, S. G.; Nair, V. B.; Siwek, C.; Patil, N. A.; Harrison, I. P.; Rosengren, K. J.; Selemidis, S.; Summers, R. J.; Wade, J. D.; Bathgate, R. A. D.; Samuel, C. S. A single-chain derivative of the relaxin hormone is a functionally selective agonist of the G protein-coupled receptor, RXFP1. *Chem. Sci.* **2016**, *7*, 3805−3819.

(20) Marshall, S. A.; O'Sullivan, K.; Ng, H. H.; Bathgate, R. A. D.; Parry, L. J.; Hossain, M. A.; Leo, C. H. B7-33 replicates the vasoprotective functions of human relaxin-2 (serelaxin). *Eur. J. Pharmacol.* **2017**, *807*, 190−197.

(21) Scott, D. J.; Rosengren, K. J.; Bathgate, R. A. D. The different ligand-binding modes of relaxin family peptide receptors RXFP1 and RXFP2. *Mol. Endocrinol.* **2012**, *26*, 1896−1906.

(22) Sethi, A.; Bruell, S.; Patil, N.; Hossain, M. A.; Scott, D. J.; Petrie, E. J.; Bathgate, R. A. D.; Gooley, P. R. The complex binding mode of the peptide hormone H2 relaxin to its receptor RXFP1. *Nat. Commun.* **2016**, *7*, 11344.
(23) Benedetti, E.; Bavoso, A.; Di Blasio, B.; Pavone, V.; Pedone, C.; Toniolo, C.; Bonora, G. M. Peptaibol antibiotics: a study on the helical structure of the 2-9 sequence of emerimicins III and IV. *Proc. Natl. Acad. Sci. U.S.A.* **1982**, *79*, 7951−7954.
(24) Doig, A. J.; Baldwin, R. L. N- and C-capping preferences for all 20 amino acids in alpha-helical peptides. *Protein Sci.* **1995**, *4*, 1325−1336.
(25) Larsen, B. D.; Jensen, L. H.; Mork, N. E.; Bjerrum, M. J.; Meissner, A.; Nielsen, G.; Jensen, P. H.; Frokjaer, S. In Structural inducing probes (SIP) - blows new hope into the general use of peptides as drugs, Peptides 2000. *Proceedings of the Twenty-Sixth European Peptide Symposium, September 10−15, 2000*, Editions EDK: Paris, France, 2001; pp 37−38.
(26) Christensen, M.; Miossec, P.; Larsen, B. D.; Werner, U.; Knop, F. K. The design and discovery of lixisenatide for the treatment of type 2 diabetes mellitus. *Expert Opin. Drug Discovery* **2014**, *9*, 1223−1251.
(27) Andrews, M. J. I.; Tabor, A. B. Forming stable helical peptides using natural and artificial amino acids. *Tetrahedron* **1999**, *55*, 11711−11743.
(28) Del Borgo, M. P.; Hughes, R. A.; Wade, J. D. Conformationally constrained single-chain peptide mimics of relaxin B-chain secondary structure. *J. Pept. Sci.* **2005**, *11*, 564−571.
(29) Kakouris, H.; Eddie, L. W.; Summers, R. J. Cardiac effects of relaxin in rats. *Lancet* **1992**, *339*, 1076−1078.
(30) Piedras-Renteria, E. S.; Sherwood, O. D.; Best, P. M. Effects of relaxin on rat atrial myocytes. I. Inhibition of I(to) via PKA-dependent phosphorylation. *Am. J. Physiol.* **1997**, *272*, H1791−H1797.
(31) Kaftanovskaya, E. M.; Soula, M.; Myhr, C.; Ho, B. A.; Moore, S. N.; Yoo, C.; Cervantes, B.; How, J.; Marugan, J.; Agoulnik, I. U.; Agoulnik, A. I. Human relaxin receptor is fully functional in humanized mice and is activated by small molecule agonist ML290. *J. Endocr. Soc.* **2017**, *1*, 712−725.
(32) Menacho-Melgar, R.; Decker, J. S.; Hennigan, J. N.; Lynch, M. D. A review of lipidation in the development of advanced protein and peptide therapeutics. *J. Controlled Release* **2019**, *295*, 1−12.
(33) Madsen, K.; Knudsen, L. B.; Agersoe, H.; Nielsen, P. F.; Thøgersen, H.; Wilken, M.; Johansen, N. L. Structure-activity and protraction relationship of long-acting glucagon-like peptide-1 derivatives: importance of fatty acid length, polarity, and bulkiness. *J. Med. Chem.* **2007**, *50*, 6126−6132.
(34) Lau, J.; Bloch, P.; Schäffer, L.; Pettersson, I.; Spetzler, J.; Kofoed, J.; Madsen, K.; Knudsen, L. B.; McGuire, J.; Steensgaard, D. B.; Strauss, H. M.; Gram, D. X.; Knudsen, S. M.; Nielsen, F. S.; Thygesen, P.; Reedtz-Runge, S.; Kruse, T. Discovery of the once-weekly glucagon-like peptide-1 (GLP-1) analogue semaglutide. *J. Med. Chem.* **2015**, *58*, 7370−7380.
(35) Bech, E. M.; Pedersen, S. L.; Jensen, K. J. Chemical strategies for half-life extension of biopharmaceuticals: lipidation and its alternatives. *ACS Med. Chem. Lett.* **2018**, *9*, 577−580.
(36) Ward, B. P.; Ottaway, N. L.; Perez-Tilve, D.; Ma, D.; Gelfanov, V. M.; Tschöp, M. H.; DiMarchi, R. D. Peptide lipidation stabilizes structure to enhance biological function. *Mol. Metab.* **2013**, *2*, 468−479.
(37) Wang, Y.; Lomakin, A.; Kanai, S.; Alex, R.; Belli, S.; Donzelli, M.; Benedek, G. B. The molecular basis for the prolonged blood circulation of lipidated incretin peptides: Peptide oligomerization or binding to serum albumin? *J. Controlled Release* **2016**, *241*, 25−33.
(38) Micsonai, A.; Wien, F.; Bulyáki, É.; Kun, J.; Moussong, É.; Lee, Y.-H.; Goto, Y.; Réfrégiers, M.; Kardos, J. BeStSel: a web server for accurate protein secondary structure prediction and fold recognition from the circular dichroism spectra. *Nucleic Acids Res.* **2018**, *46*, W315−W322.

https://dx.doi.org/10.1021/acs.jmedchem.0c01533
J. Med. Chem. 2021, 64, 2139−2150